Correlation Hole Effect in Comblike Copolymer Systems Obtained by Hydrogen Bonding between Homopolymers and End-Functionalized Oligomers

J. Huh,[†] O. Ikkala,[‡] and G. ten Brinke*[,†,‡]

Materials Science Center, Department of Polymer Science, University of Groningen, Nijenborgh 4, 9747 AG Groningen, The Netherlands, and Materials Physics Laboratory, Department of Technical Physics, Helsinki University of Technology, Rakentajanaukio 2, FIN-02150 Espoo, Finland

Received September 26, 1996; Revised Manuscript Received December 23, 1996[⊗]

ABSTRACT: This paper addresses concentration fluctuations in comblike copolymer systems obtained by hydrogen bonding between polymers and end-functionalized oligomers. Monodisperse block copolymer systems in the homogeneous melt exhibit small-angle X-ray scattering peaks at finite nonzero angle due to characteristic correlation hole concentration fluctuations. In comblike copolymer systems obtained by hydrogen bonding, the dominant fluctuations have been found by us to vary experimentally between conventional long wavelength fluctuations (for weak hydrogen bonding) and finite wavelength fluctuations (strong hydrogen bonding). Monte Carlo computer simulations show that both regimes occur in one and the same system depending on the temperature. The transition between both regimes is directly related to the fraction of free oligomers, which depends on the temperature and the interactions. The structure factors are analyzed in terms of the random phase approximation applied to a mixture of free oligomers and comb copolymers, using a uniform distribution of teeth along the polymer chains and a binomial distribution in the number of polymers with a given number of teeth, confirmed numerically, as input. The agreement is excellent at both high and low temperatures.

Introduction

In recent years, it has been demonstrated that noncovalent bonds can be used advantageously in creating very well ordered nanostructures and that the concept can be applied for various applications such as for instance the molecular construction of polymer liquid crystals. They can involve hydrogen bonds, ionic interactions, coordination complexes, charge-transfer interactions, etc.[1−6] Besides charge transfer[7] and coordination complexation,[8] we have studied extensively polymer−surfactant systems involving hydrogen bonds.[9−12] Poly(4-vinylpyridine) (P4VP) was used as a model polymer in combination with various end-functionalized oligomers. The latter consist of a long alkyl tail and a functional head group which can make a hydrogen bond with the nitrogen of the pyridine groups of P4VP. All systems studied involved polymers and short-chain molecules only; no additional low molecular weight solvent was present. Because of this fact and the long flexible tail of the oligomers, these systems can be discussed, at least in a first approximation, in terms of random walk chain statistics and the random phase approximation.[13]

If the hydrogen-bonding interaction is rather strong, the polymer structures resemble in many ways conventional comb copolymers. In this case, the system is either homogeneous, micro-phase separated, or possibly even macro-phase separated. For the particular system of P4VP and pentadecylphenol (PDP), a homogeneous state was observed at elevated temperatures, i.e. above 70 °C. Upon cooling, an order−disorder transition from a homogeneous to a micro-phase-separated state was observed at a temperature depending on the composition of the system.[9,12] Macro-phase separation has not been observed so far; however, it is believed that if macro-phase separation occurs, this will happen for a large excess of oligomers, a situation not yet studied experimentally. With respect to the present paper, the most important observation is the occurrence of a scattering peak at finite nonzero scattering vector in the homogeneous state. So, the hydrogen bonds between the phenol groups of the oligomers and the pyridine groups of the polymers are apparently strong enough to give rise to the correlation hole effect.[13−15]

It is well known that the hydrogen-bonding capability of aliphatic alcohols is far less than for phenols. Experimentally, we observed that P4VP and dodecanol still form homogeneous mixtures in the temperature range studied. However, the shape of the scattering curve now resembles the scattering curve of ordinary binary mixtures, i.e. a small-angle scattering that decreases monotonously as a function of the wave vector. The correlation hole effect is no longer present.[10] For aliphatic alcohols with even longer alkyl tails, macro-phase separation occurs due to the unfavorable alkyl−polymer interactions which are no longer compensated by the weak hydrogen-bonding interaction.

These experimental observations demonstrate that the nature of the concentration fluctuations in the homogeneous state of these type of polymer−surfactant systems can be quite different. For weak hydrogen bonding a conventional binary mixture behavior is observed, whereas for strong hydrogen bonding a comb copolymer-like behavior is observed. In the latter case, a transition from strong to weak hydrogen-bonding behavior should occur at elevated temperatures. However, in practice this has not been observed so far and, consequently, no experimental information related to the transition between these two extremes is available. It is precisely this issue that is addressed in this paper. Using a simplified lattice model, we will demonstrate that a decrease in the temperature leads to a sudden manifestation of the correlation hole effect. These facts are then backed up by theoretical calculations.

[†] University of Groningen.
[‡] Helsinki University of Technology.
[⊗] Abstract published in *Advance ACS Abstracts,* March 1, 1997.

S0024-9297(96)01439-8 CCC: $14.00

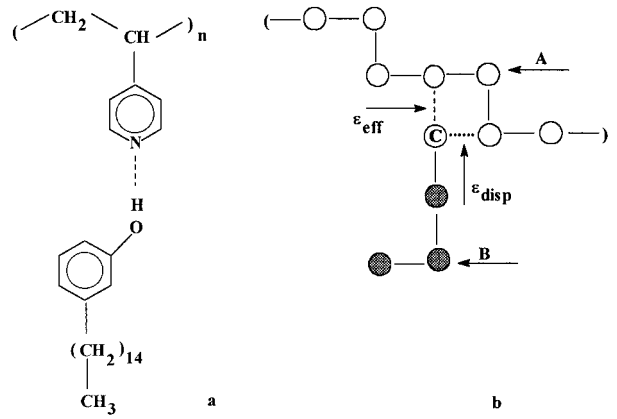

Figure 1. (a) P4VP−PDP hydrogen bond. (b) Schematic lattice model; ϵ_{eff} corresponds to ϵ_{disp} or ϵ_{hb} according to the principles outlined in the text.

Computer Simulation Model

In order to study the appearance of a correlation hole effect due to specific interactions we use Monte Carlo simulations on a model inspired by the polymer/end-functionalized oligomer systems studied experimentally. The simulated system consists of a $40 \times 40 \times 40$ cubic lattice model and contains chains P(A) of length 32 and oligomers P(B)−C of length 4; here A denotes the segments of the polymer, C the functional head group of the oligomer, and B the segments of the oligomer tail. The volume fraction of both constituents is 0.4, leaving a volume fraction of voids equal to 0.2.

The model incorporates a number of features that are essential to systems involving hydrogen bonds (cf. Figure 1a).[16−18] Hydrogen bonding is extremely directional specific with angular spreads of 10° at most. If the relative orientation of the two groups involved changes with more than 10°, the bond will break and be replaced by a dispersive interaction. Hence, two adjacent groups that can form a hydrogen bond will very often not be in the right position to do so. In our model, a segment of the polymer chain and the functional head group of a oligomer can form at most one hydrogen bond. For the oligomer this is accomplished by assuming that the functional head group can make a hydrogen bond with a neighboring polymer segment only if the latter is located in the direction of the bond connecting the head with its preceding tail segment (Figure 1b). For the polymer segments it has to be introduced as a constraint. Now, even if a polymer segment and a functional head group are in the right position with respect to each other, the automatic assignment of a hydrogen bond will still considerably overestimate the hydrogen bond formation probability. Therefore, an adjustable parameter q is introduced: if a polymer segment and a functional head group are in a position with respect to each other which in principle allows a hydrogen bond to be formed, both groups involved have still so much freedom that out of $q + 1$ "intrinsic" states of the segment pair only 1 actually corresponds to a hydrogen bond. In the past this kind of modeling has been applied rather successfully to hydrogen-bonding systems.[16−19]

In our model we will assume that all non-hydrogen-bonding interactions between unlike segments are equal and denote it by ϵ (>0). Furthermore, the hydrogen bond interaction is denoted by ϵ_{hb} (<0). The interaction between segments of the same kind equals 0. On the basis of these assumptions the system is characterized by an effective hydrogen-bonding interaction ϵ_{eff} given by

$$\epsilon_{eff} = \lambda\epsilon_{hb} + (1 - \lambda)\epsilon \tag{1}$$

where

$$\lambda = [q\, exp\Delta\epsilon' + 1]^{-1} \tag{2}$$

$\Delta\epsilon = \epsilon_{hb} - \epsilon$ and $\Delta\epsilon' = \Delta\epsilon/kT$. Equation 2 represents the fraction of hydrogen bonds that are actually formed once the surfactant head and a polymer segment are in a suitable position. The introduction of the parameter q, leading to this expression, takes care of the well-known fact that the number of hydrogen bonds becomes extremely small in the high-temperature limit, provided $q \gg 1$. In the simulations we will take $q = 10$. For elevated temperatures the dispersive forces dominate and ϵ_{eff} may even become positive. This fact is responsible for macro-phase separation often observed in "ordinary" mixtures with hydrogen-bonding interactions (i.e. water/tetrahydrofuran, poly(ethylene oxide)/water, etc.[20,21]). In that case, usually closed-loop phase diagrams are found due to re-entrant miscibility at high temperatures where the entropy of mixing dominates.[16,17] Our results will be presented as a function of $N\epsilon'$, where N equals the average number of segments per "comb copolymer" in the limit of infinitely strong hydrogen bonding and $\epsilon' = \epsilon/kT$. Furthermore,

$$\epsilon_{hb} = -R\epsilon \tag{3}$$

where R is used as a material parameter expressing the relative strength of the hydrogen bond in relation to the dispersive interaction. There are two more variables to be introduced, x, representing the molar ratio between the number of oligomers and the total number of polymer segments (i.e. actually the ratio between the number of complementary functional units), and L, denoting the molecular length ratio between polymer chain and oligomer. Table 1 summarizes the values of the main parameters used in the present study.

Table 1

lattice size L_s	40[a]
length of polymer N_A	32[a] ($[A]_{32}$)
length of oligomer $N_B + N_C$	4[a] ($[B]_3-[C]_1$)
no. of polymers n_p	800 and 320[b]
no. of oligomers n_s	6400 and 10240[b]
fraction of voids ϕ_v	0.2

[a] Unit of lattice spacing. [b] Can be varied depending upon $x = n_s/n_pN_A$ and $L = N_A/(N_B + N_C)$; in the table, the numbers are for $x = 0.25$ and $x = 1.0$, respectively, $L = 8$.

The molecules are in a cubic simulation box with periodic boundary conditions and move by "slithering snake algorithm",[22] and the configurational space is sampled by Metropolis importance sampling,[23] which is performed by checking the energy of the system given by

$$E = kT[(n_{AB} + n_{BC} + n_{AC})\epsilon' + n_s(1 - \phi_{fs})\epsilon'_{hb}] \tag{4}$$

where n_{AB} and n_{BC} are the number of contacts between the segments indicated and n_{AC} is the number of contacts between segments A and C that are in a nearest-neighboring position without hydrogen bonding. $1 - \phi_{fs}$ is the fraction of oligomers involved in hydrogen bonding. ϕ_{fs} is the fraction of "free" oligomers.

The structure factors are calculated by spherical and thermal averaging, i.e.

$$S_{AA}(k) = \langle \sum_{m,n} e^{ik\cdot(rm-rn)} \Psi_A(r_m)\Psi_A(r_n)\rangle \quad (5)$$

$$S_{AA}(k) = \sum_{|k|=k} S_{AA}(k) / \sum_{|k|=k} 1 \quad (6)$$

where $\Psi_A(r)$ is $1 - \phi_A$ or $-\phi_A$ depending on whether an A segment is at $\vec{r}$ or not. Thermal averaging $\langle\ \rangle$ was taken over 200 independent configurations. In the results reported here, $R = 20$ and ϵ' varies from 2/64 to 16/64 with steps of 2/64. In the present paper, the emphasis is on the correlation hole effect in the homogeneous state and R is not varied. However, to study the possibility of macro-phase separation, smaller values of $R \cong 5$ are required.[24]

Theoretical Modeling

The structure factor of comb copolymers has been addressed in the past by various groups. Benoit and Hadziioannou[15] considered the case of comb copolymers with the teeth equally spaced along the backbone. Polydispersity was considered, but only with respect to the length of the polymer backbone and the length of the teeth. A more comprehensive treatment of polydispersity was given by Balazs and co-workers.[25] They considered and analyzed three models for comb copolymers, allowing for randomness in the placement and number of teeth. In our case, we are dealing with comblike copolymer structures consisting of polymer, hydrogen-bonded functional oligomers, and free oligomers. To compare the numerical results with theoretical predictions we will treat the system on the basis of assumptions which seem not only reasonable but which are also confirmed by the computer simulations. The polymer/oligomer system is treated as a mixture of polydisperse comb copolymers (polydisperse in terms of the number and placement of "teeth") and free oligomer molecules. In terms of this model, we will only distinguish two types of segments, A of the backbone polymer and B of the teeth and the free oligomer. Furthermore, the random phase approximation will be employed (even though in the simulations the oligomer molecules are rather short), implying that the structure factor, $S(k)$, can be obtained in terms of response functions of the intramolecular correlation of ideal Gaussian chains. The essential input concerns the polydispersity in terms of number and placement of teeth. As confirmed by the computer simulations, the positions of the teeth along the polymer chains are uncorrelated, and the distribution of polymers having n_t teeth, $P(n_t)$, can be described by a binomial distribution.

According to the random phase approximation, the structure factor $S(k)$ of the system is given by

$$S(k) = \frac{1}{\Gamma(k) - 2\chi} \quad (7)$$

where

$$\Gamma(k) = \frac{S_{AA} + S_{BB} + 2S_{AB}}{S_{AA}S_{BB} - S_{AB}^2} \quad (8)$$

χ is the Flory−Huggins interaction parameter between A and B segments, $S_{\alpha\beta}$ is the second-order correlation function between monomers α (A or B) and β (A or B) averaged over all different molecule types in the system, implying

$$S_{\alpha\beta} = \sum_s \rho_s g^s_{\alpha\beta} \quad (9)$$

where ρ_s is the number density expressed as number of molecules type s in a given volume ($\sum_s \rho_s N_s = 1$, where N_s denotes the number of segments of molecule of type s), and $g^s_{\alpha\beta}$ is the second-order correlation function of molecule of type s. Then the $S_{\alpha\beta}$ for this particular system are given by

$$S_{AA} = \rho_p \sum_{n_t} P(n_t) \int_0^{N_A}\int_0^{N_A} e^{-y|i-j|}\, di\, dj \quad (10)$$

$$S_{AB} = \rho_p \sum_{n_t} P(n_t) \int_0^{N_B} e^{-ym}\, dm \int_0^{N_A}\int_0^{N_A} P_t(i) e^{-y|i-j|}\, di\, dj \quad (11)$$

$$S_{BB} = \rho_{fs}\int_0^{N_B}\int_0^{N_B} e^{-y|i-j|}\, di\, dj + \rho_p \sum_{n_t} [P(n_t)\{n_t \int_0^{N_B}\int_0^{N_B} e^{-y|i-j|}\, di\, dj + (\int_0^{N_B} e^{-ym}\, dm)^2 \int_0^{N_A}\int_0^{N_A} P_t(i,j) e^{-y|i-j|}\, di\, dj\}] \quad (12)$$

where in eq 12 the first term represents the correlation within free oligomer molecules and the second term contains two contributions, one due to the correlation within the same tooth and between two different teeth within the same polymer. ρ_s is the number density of molecules of type s with s = p referring to polymer and s = fs to free oligomer. N_A is the length of the polymer, N_B is the length of the oligomer molecule, and $y = k^2a^2/6$, where a is the segment size and k the scattering vector. Furthermore, n_t is the number of teeth of a particular polymer backbone, and $P(n_t)$ is the probability of finding a polymer which has n_t teeth. $P_t(i)$ denotes the probability of finding a tooth at the position of the ith monomer along the polymer backbone, whereas, $P_t(i,j)$ denotes the probability of finding simultaneously teeth at the position of the ith and jth monomers ($i \neq j$) of a polymer backbone.

Assuming that the teeth on a polymer backbone are uncorrelated, $P_t(i)$ and $P_t(i,j)$ are simply given by the uniform distribution;, hence:

$$P_t(i) = \frac{n_t}{N_A} \qquad P_t(i,j) = \frac{n_t}{N_A}\frac{n_t - 1}{N_A - 1} \approx \frac{n_t(n_t-1)}{N_A^2} \quad (13)$$

Inserting eq 13 into eqs 9−12 and performing integration lead to

$$S_{AA} = \frac{2\rho_p}{y^2}[N_A y + e^{-N_A y} - 1] \quad (14)$$

$$S_{AB} = \frac{2\rho_p\langle n_t\rangle}{N_A y^3}[1 - e^{-N_B y}][N_A y + e^{-N_A y} - 1] \quad (15)$$

$$S_{BB} = \frac{2}{y^2}[\rho_{fs} + \langle n_t\rangle\rho_p][N_B y + e^{-N_B y} - 1] + \frac{2\rho_p}{N_A^2 y^4}[\langle n_t^2\rangle - \langle n_t\rangle][1 - e^{-N_B y}]^2[N_A y + e^{-N_A y} - 1] \quad (16)$$

where $\langle n_t\rangle = \sum_{n_t} n_t P(n_t)$. The probability of finding a tooth

at a given polymer segment position is $p = \langle n_t \rangle / N_A$. If the positions of the teeth are uncorrelated, the distribution function $P(n_t)$ for a polymer to have n_t teeth is simply given by the binomial distribution

$$P(n_t) = \binom{N_A}{n_t} \left[\frac{\langle n_t \rangle}{N_A}\right]^{n_t} \left[1 - \frac{\langle n_t \rangle}{N_A}\right]^{N_A - n_t} \quad (17)$$

Then we can estimate $\langle n_t^2 \rangle$ from

$$\langle n_t^2 \rangle = \sum_{n_t} n_t^2 P(n_t) = \langle n_t \rangle^2 + \langle n_t \rangle \left[1 - \frac{\langle n_t \rangle}{N_A}\right] \quad (18)$$

If there are no free oligomers in the system, which is only possible as long as $x \leq 1$, $P(n_t)$ and $\langle n_t^2 \rangle$ are given by

$$P(n_t) = \binom{N_A}{n_t} [x]^{n_t} [1 - x]^{N_A - n_t} \quad (19)$$

$$\langle n_t^2 \rangle = N_A^2 x^2 + N_A x(1 - x) \quad (20)$$

In the following section we will compare these theoretical predictions for the structure factor and for the polydispersity of the comb copolymers with our numerical simulation results. In order to achieve this, the numerically obtained values for $\langle n_t \rangle$ and $\langle n_t^2 \rangle$ will be taken as input values for eqs 15 and 16.

Whether or not a scattering peak occurs at a finite nonzero value ($k^* \neq 0$) of the scattering vector k depends on the average number of side chains per molecule. It is rather straightforward to derive an equation for the transition from $k^* = 0$ to $k^* \neq 0$ by realizing that this transition point corresponds to

$$\frac{\partial \Gamma(y=0)}{\partial y} = 0 \quad (21)$$

This results in

$$(N_A - 1)\langle n_t \rangle^4 + (3 + 2L)N_A \langle n_t \rangle^3 + \left(N_A L^2 + 3N_A L + 2N_A^2 x + \frac{2N_A^2}{L} x\right)\langle n_t \rangle^2 + N_A^3 x \langle n_t \rangle - N_A^3 x(L + N_A x) = 0 \quad (22)$$

The physical root of this equation gives the critical value $\langle n_t \rangle^c$ of $\langle n_t \rangle$ and thus the critical ratio of free oligomers: $n_{fs}^c/n_s = (N_A x - \langle n_t \rangle^c)/(N_A x)$. In the region where $\partial\Gamma(y=0)/\partial y > 0$, the dominant scattering vector $k^* = 0$, whereas in the region where $\partial\Gamma(y=0)/\partial y < 0$, $k^* \neq 0$. Figure 2 shows the theoretical prediction for $L = 8$ and $N_A = 32$, the values most frequently used in our computer simulations.

Computer Simulation Results

In ref 15 the structure factor of comb copolymers with equally spaced teeth was derived. Denoting the number of segments for the backbone by N_A and for the side chains by N_B, the structure factor for the pure monodisperse comb copolymer melt was found to have its maximum for

$$k^2 \langle r^2 \rangle \cong 4 \quad (23)$$

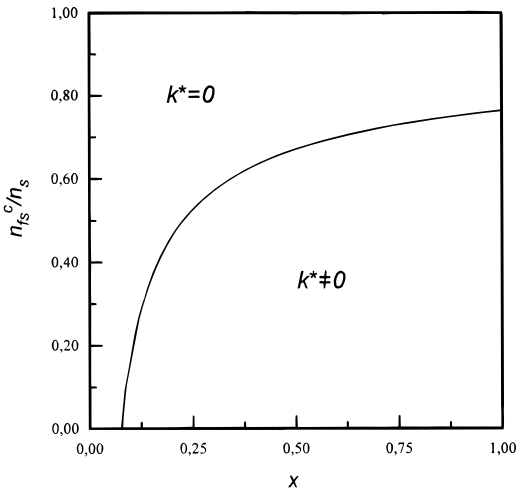

Figure 2. Critical fraction of free oligomers, n_{fs}^c/n_s, at the transition between the situation characterized by a structure factor decreasing monotonously as a function of scattering angle ($k^* = 0$) and the situation characterized by a scattering peak at finite nonzero angle ($k^* \neq 0$) as a function of the amount of oligomer x ($=n_s/(N_A n_p)$). $N_A = 32$, $L = 8$.

where

$$\langle r^2 \rangle = \left(\frac{N_A}{n_t} + N_B\right) a^2 \quad (24)$$

where n_t is the number of teeth per comb copolymer and, hence, N_A/n_t is the number of segments in between the equally spaced teeth. Equations 23 and 24 demonstrate that, as to be expected, the correlation hole extends over a distance that corresponds to the size of the characteristic building block of these structures.

To compare our computer simulations result with these predictions, the structure factor will be presented as a function of a variable z_0, which will be defined in the limit of no free oligomers as the analogy of the left-hand side of eq 23. In this limit the following expression for the total number of teeth $n_{t,0}$ per polymer holds:

$$n_{t,0} = \frac{n_s}{n_p} = x N_A \quad (25)$$

Furthermore, n_0 is defined by

$$n_0 = \frac{N_A}{n_{t,0}} + N_B \quad (26)$$

The variable z_0 is now given by

$$z_0 = y n_0 = \frac{k^2 a^2 n_0}{6} = k^2 r^2 \quad (27)$$

where r is the radius of gyration of the characteristic subunit of our structures in the limit of infinitely strong hydrogen bonding, i.e. no free oligomers.

We will start by considering in detail the case of $x = 0.25$. Thereafter, the case of $x = 1.0$ will be considered briefly. The main results of our computer simulations are presented in Figure 3, where the numerical structure factors are given as a function of the scattering vector expressed in terms of z_0, for a range of values of the dispersive interaction ϵ', the hydrogen-bonding interaction being given by eq 3, with $R = 20$. Around $N\epsilon' = 10$, the structure factor starts to develop a peak

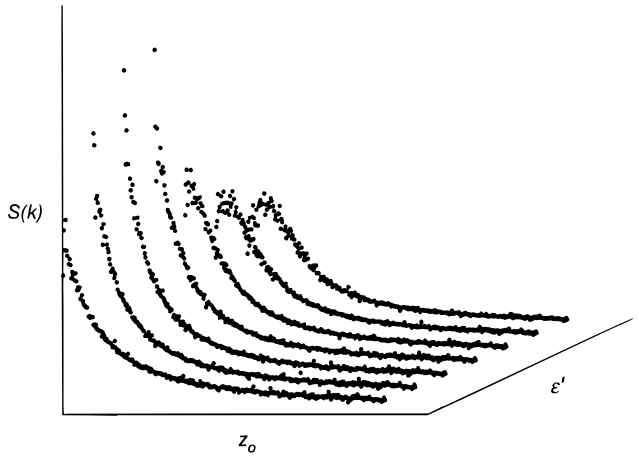

Figure 3. Structure factors obtained by computer simulations $\{N_A = 32, x = 0.25, L = 8, N = 64, N\epsilon' = 2, 4, 6, 8, 10, 12, 14, R = 20, q = 10\}$.

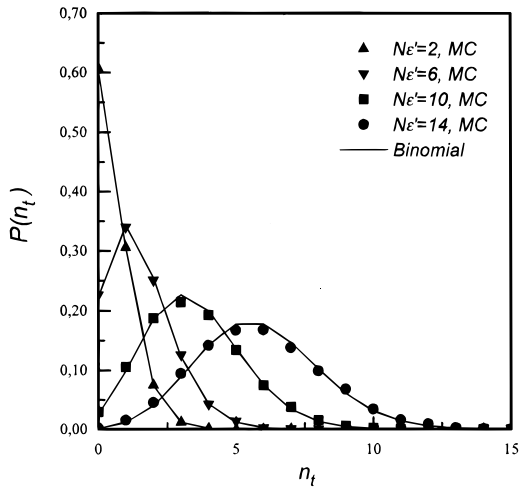

Figure 4. Probability $P(n_t)$ for the polymer backbone to have n_t teeth as a function of the interaction $N\epsilon'$. $x = 0.25$, $N = 64$, $N_A = 32$, $L = 8$, $R = 20$, $q = 10$. The data points represent computer simulation data. The line represents the binomial result eq 17 with $\langle n_t \rangle$ taken from the simulation.

at nonzero scattering vector. Below this value, it is a monotonously decreasing function of the scattering vector, whereas for larger values a pronounced peak appears. Before we address this further, the nature of the comblike copolymer structures will be considered in more detail first.

Figure 4 presents the probability $P(n_t)$ that a particular structure possesses n_t teeth, where the teeth are formed by the oligomers that have actually formed a hydrogen bond with the polymer. Besides the computer simulation data, the figure also contains the probability calculated on the basis of the binomial expression eq 17 using the average number of teeth $\langle n_t \rangle$ obtained by the simulations as input. The binomial distribution follows from the assumption that the positions of the teeth along the polymer backbones are uncorrelated, a property that is clearly confirmed by the numerical data. The experimental results for the P4VP−PDP system seem to confirm this as well.[9] For a similar comblike copolymer system based on ionic interactions, P4VP and *p*-dodecylbenzenesulfonic acid (DBSA), the experimental results clearly indicate cooperativity. Successive teeth seem to prefer nearest-neighbor pyridine groups. This is also the case for P4VP complexed with zinc dodecylbenzenesulfonate ($Zn(DBS)_2$). In this case, there are no covalent bond charges along the polymer backbone, but

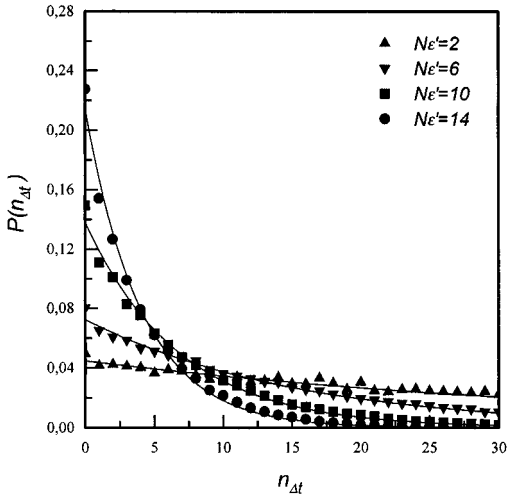

Figure 5. Probability $P(n_{\Delta t})$ of finding $n_{\Delta t}$ polymer segments in between two consecutive teeth as a function of the interaction $N\epsilon'$. $x = 0.25$, $N = 64$, $N_A = 32$, $L = 8$, $R = 20$, $q = 10$. The data points represent computer simulation data. The solid line represents a fit using an exponential decay function.

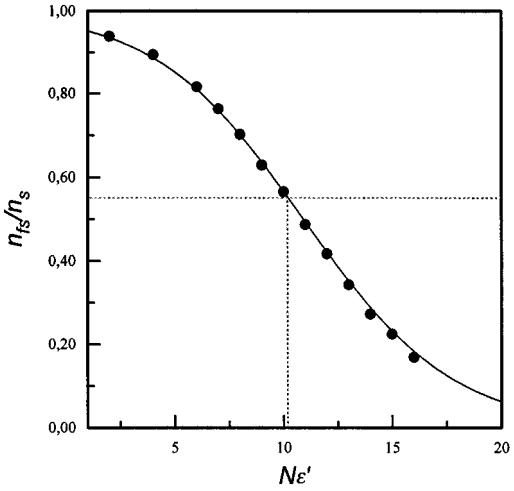

Figure 6. Fraction of free oligomers n_{fs}/n_s as a function of $N\epsilon'$. $x = 0.25$, $N = 64$, $N_A = 32$, $L = 8$, $R = 20$, $q = 10$. Data points correspond to the computer simulations. The curve is a fit based on Tanaka's theory.[30] The horizontal dotted line corresponds to the critical value n_{fs}^c/n_s for the appearance of a correlation hole peak as it follows from the theoretical results presented in Figure 2.

there are still ionic charges complexed to the polymer because of the ionic zinc sulfonate salt. Hence, it seems that cooperative complexation is directly related to the presence of charges.[9]

Figure 5 presents the probability $P(n_{\Delta t})$ of having $n_{\Delta t}$ backbone segments between two consecutive teeth. The exponential behavior is exactly as expected from a uniform distribution.

From the theoretical results in the last section we know that for $x = 0.25$, the appearance of a scattering peak at nonzero wave vector should occur once the fraction of free oligomers falls below 0.55. Figure 6 presents the numerical result for this fraction n_{fs}/n_s as a function of $N\epsilon'$ and shows that this also occurs for $N\epsilon' \cong 10$. The solid line is a theoretical fit based on a recent theory put forward by Tanaka.[29,30]

Having established the polydispersity of the comb copolymer structures, we proceed with a detailed comparison between the structure factors obtained by the computer simulations and by the theoretical description based on the random phase approximation. Figure 7

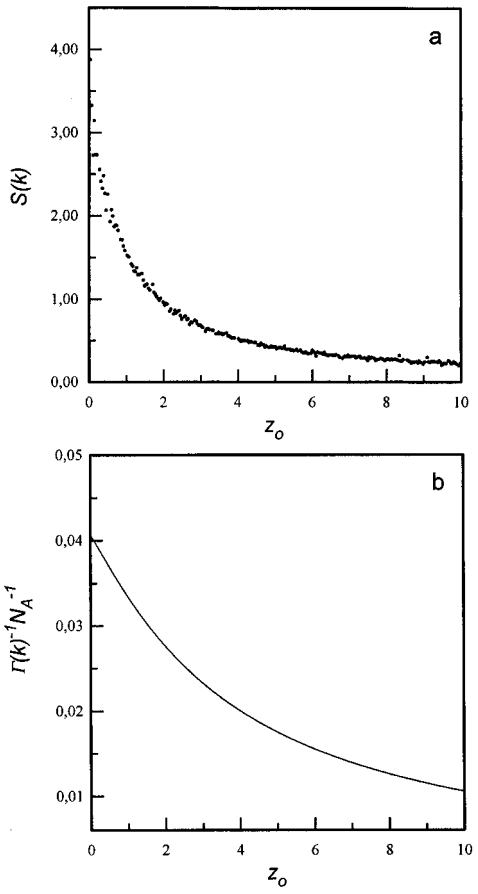

Figure 7. (a) Structure factor from computer simulation for $N\epsilon' = 6$. (b) Calculated structure factor using $\langle n_t \rangle = 1.47$ and $\langle n_t^2 \rangle = 3.56$. $x = 0.25$, $N = 64$, $N_A = 32$, $L = 8$, $R = 20$, $q = 10$.

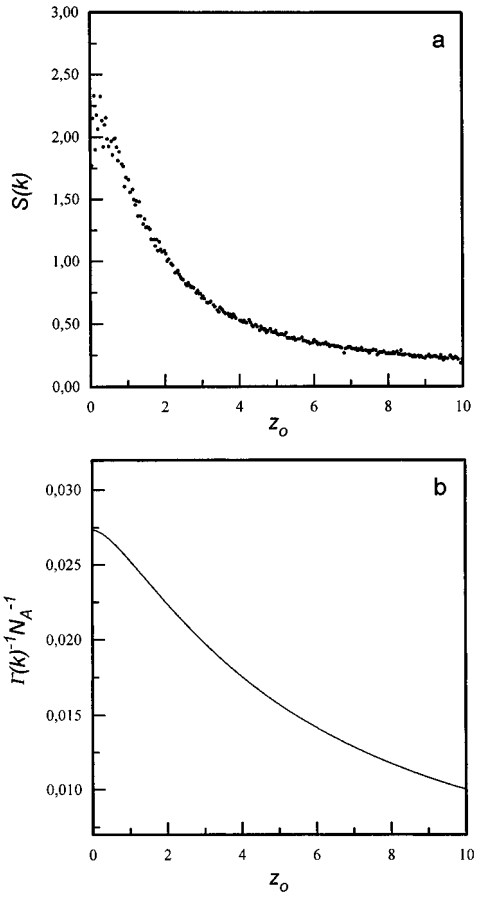

Figure 8. (a) Structure factor from computer simulation for $N\epsilon' = 10$. (b) Calculated structure factor using $\langle n_t \rangle = 3.48$ and $\langle n_t^2 \rangle = 15.19$. $x = 0.25$, $N = 64$, $N_A = 32$, $L = 8$, $R = 20$, $q = 10$.

presents this comparison between the numerically obtained structure factor for $N\epsilon' = 6$ and the theoretically calculated $1/\Gamma(k)$ using eqs 8 and 14−16. Since we are interested in the transition from a situation where the structure factor is dominated by long wavelength fluctuations to a situation characterized by a typical correlation hole peak, we restrict ourselves to theoretical calulations based on $\chi = 0$. Theoretically, positive values of χ only enhance the peak height but do not change its position. The calculated curve uses as input values $\langle n_t \rangle = 1.47$ and $\langle n_t^2 \rangle = 3.56$ obtained by the computer simulations. Clearly, both curves are very similar and represent monotonously decreasing functions.

Reducing the temperature leads to larger values of ϵ' and ultimately to a manifestation of the correlation hole effect in the form of a scattering peak at finite nonzero wave vector. Figure 8 presents the result for $N\epsilon' = 10$. At this value, the numerical data indicate the development of a peak at very small angle. The theoretically calculated curve, which is based on $\langle n_t \rangle = 3.48$ and $\langle n_t^2 \rangle = 15.19$, shows a similar peak development at zero angle. In this particular case, the numerical results are obviously influenced by finite size effects, since the long wavelength fluctuations exceed the size of our simulation box. Still the agreement between the theory and the computer simulations, as far as the development of a scattering peak at finite scattering angle is concerned, is more than satisfactory.

For still lower temperatures or larger values of ϵ', the situation becomes more clear. Figure 9 presents the data for $N\epsilon' = 14$. The computer simulation data now show a definite peak at finite nonzero angle and the theoretically calculated data, based on $\langle n_t \rangle = 5.82$ and $\langle n_t^2 \rangle = 38.67$, are in excellent agreement with this observation. The size of the simulation box is now much larger than the wave vector corresponding to the peak in the structure factor.

Figure 10 presents the theoretical curves when no free surfactant is left, in which case $\langle n_t \rangle = 8.0$ and $\langle n_t^2 \rangle = \Sigma n_t^2 P(n_t) = 70.0$ (based on eq 17). Figure 10a corresponds as before to $N_A = 32$. The peak occurs at $z_0 \cong 1.6$. In the case of equally spaced teeth, the theoretical predictions given by Benoit and Hadziioannou[15] amount to $z_0 \cong 4.0$. Hence, as might be expected, the polydispersity in the position of the teeth along the backbone and in number of teeth per polymer chain results in a shift of the scattering peak to a much smaller angle. From eq 20, we see that for a given value of xN_A, the polydispersity (i.e. σ^2) increases for increasing backbone length N_A. As a consequence, the peak position will shift to even smaller angles as illustrated in Figure 10b. Of course, this effect of polydispersity has been found also by other groups.[15,25]

Finally, we consider briefly the case of $x = 1.0$, all other parameters being unchanged. Figure 11 presents the numerically obtained structure factors for $N\epsilon' = 2$, 4, ..., 14, with $N = 64$. As before, a correlation hole peak starts to develop at $N\epsilon' \cong 10$. From Figure 2 we know that theoretically the appearance of a peak at finite nonzero angle should occur once $n_{fs}^c/n_s \cong 0.77$. Figure 12 presents the numerical data of the ratio n_{fs}/n_s as a function of $N\epsilon'$ for $x = 1$ and demonstrates that $n_{fs}/n_s \cong 0.77$ also occurs at $N\epsilon' \cong 10$. The situation is

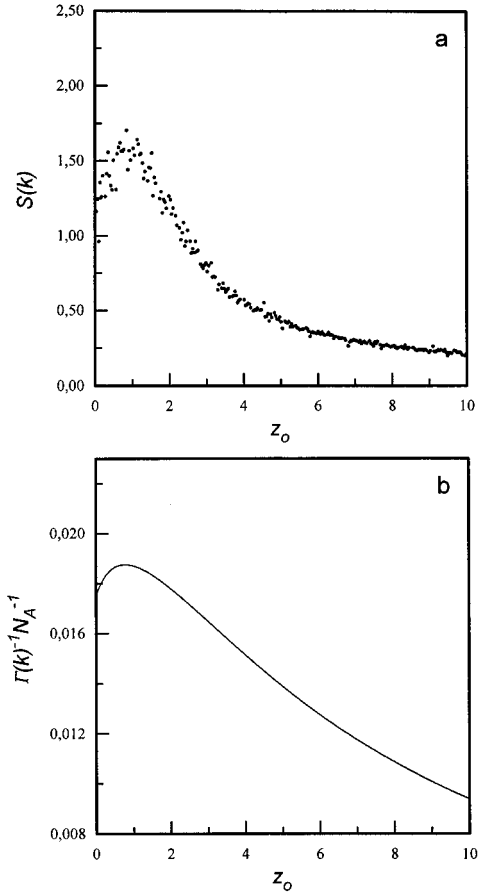

Figure 9. (a) Structure factor from computer simulation for $N\epsilon' = 14$. (b) Calculated structure factor using $\langle n_t \rangle = 5.82$ and $\langle n_t^2 \rangle = 38.67$. $x = 0.25$, $N = 64$, $N_A = 32$, $L = 8$, $R = 20$, $q = 10$.

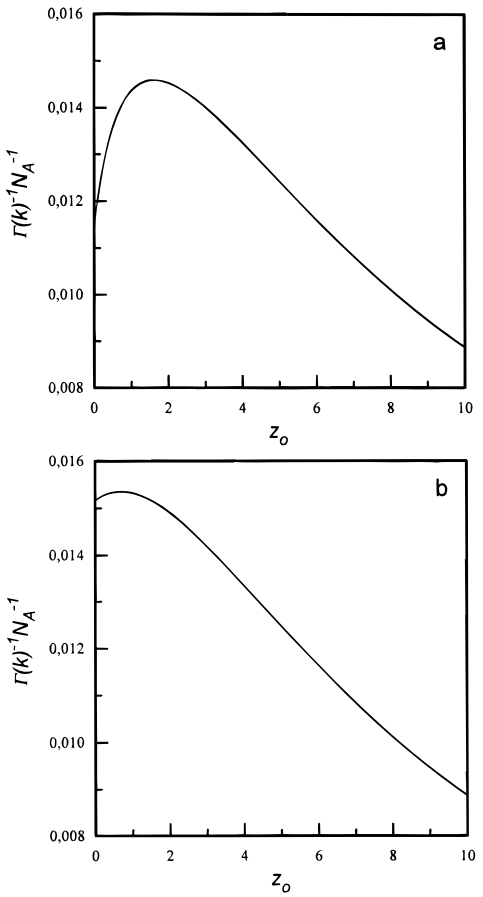

Figure 10. Theoretical structure factor in the limit $n_{fs} = 0$: (a) $N_A = 32$, $x = 0.25$; (b) $xN_A = 8$, $N_A \rightarrow \infty$. $L = 8$, $R = 20$, $q = 10$.

similar to $x = 0.25$, with the notable exception that the development of a correlation hole peak starts when a much larger fraction of the oligomers is still free. At low temperatures, where hydrogen bonding dominates, nearly all segments of the polymers will be hydrogen bonded with the functional oligomers. In this case the polydispersity disappears, in contrast to the $x = 0.25$ situation.

Concluding Remarks

In the previous sections we addressed the manifestation of the correlation hole effect in polymer−surfactant systems, where the surfactant is an end-funtionalized oligomer, using Monte Carlo computer simulations. The model incorporated the directional specific nature of hydrogen bonding by introducing an entropy penalty for the formation of a hydrogen bond between the oligomer head groups and the polymer segments which are in a position allowing a hydrogen bond to be formed. Using this formalism, we demonstrated that the correlation hole effect can be explained by treating all polymer−oligomer complexes as "permanent" comb copolymers. Still, this is not entirely trivial because it implies that all oligomers that interact with the polymer are treated as permanent side chains, whereas those oligomers that are in an identical position without hydrogen bonding (due to q) are treated as free. The sudden manifestation of the correlation hole effect on reducing the temperature (increasing ϵ') is due to the fraction of free oligomers decreasing below a critical value. It is quite obvious that this observation should apply to our experimentally investigated P4VP−alkyl alcohols as well.

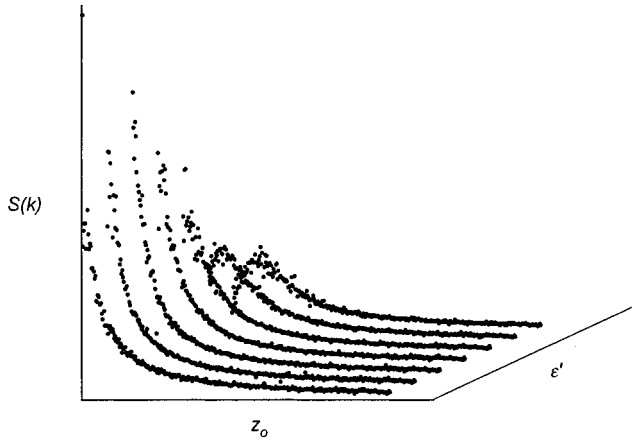

Figure 11. Structure factors obtained by computer simulations {N_A=32, $x = 1.0$, $L = 8$, $N = 64$, $N\epsilon' = 2$, 4, 6, 8, 10, 12, 14, $R = 20$, $q = 10$}.

Very recently, a related computer simulation study appeared,[26] dealing with solutions of telechelic chains with strongly attracting end groups. Because the end groups are allowed to interact strongly with more than one group at the same time, the authors actually study the formation of micelles and micellar gel-like structures. They find a pronounced maximum in the structure factor attributed to a quasiperiodic pattern of alternating microdomains consisting of dense micellar cores and swollen soluble chain blocks. Our experimental work, discussed in this paper, concerned functionalities (hydrogen bonding) restricting the number of strong interactions to one per group. However, preliminary measurements involving P4VP and oligomers

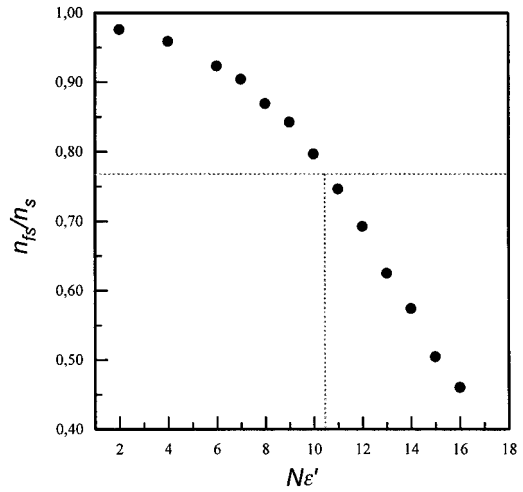

Figure 12. Fraction of free oligomers n_{fs}/n_s as a function of $N\epsilon'$. $x = 1.0$, $N = 160$, $N_A = 32$, $L = 8$, $R = 20$, $q = 10$. Data points correspond to the computer simulations. The horizontal dotted line corresponds to the critical value n_{fs}^c/n_s for the appearance of a correlation hole peak as it follows from the theoretical results presented in Figure 2.

capable of several hydrogen bondings, i.e. 1-dodecyl 3,4,5-trihydroxybenzoate, have already been performed. In this case, micro-phase separation was observed at all temperatures, characterized by a pronounced scattering peak.[27] However, the emphasis in the present paper is on the development of a scattering peak at finite nonzero angle in the *homogeneous* state due to the correlation hole effect, rather than micro-phase-separated structures.

An even more closely related paper was published by Nose and co-workers.[28] They addressed experimentally the association between one-end-animated polystyrene and one-end-carboxylated or -sulfonated poly(ethylene glycol). Many features observed are similar to our observation for the polymer-end-functionalized oligomer systems, including a correlation hole effect for strong enough association.

Theoretically, phase behavior in strongly associating systems has been studied in detail by Tanaka and co-workers.[30−32] In their most recent paper,[30] inspired by our experimental results, the authors address the phase behavior of the same class of comblike copolymers as studied in this paper. The phase diagram presented shows a number of interesting features not present in ordinary comb copolymer systems due to the reversibility of the association. However, many questions still remain unanswered because of a lack of understanding concerning the precise nature of the micro-phase-separated structures formed.

Acknowledgment. Useful discussions with Henk Angerman during the course of this work as well as with Prof. A. R. Khokhlov and Dr. E. Dormidontova during the final stage of this work are gratefully acknowledged. We would also like to thank Prof. F. Tanaka for sending us a preprint of his work prior to publication.

References and Notes

(1) Lehn, J.-M. *Makromol. Chem., Macromol. Symp.* **1993**, *69*, 1.
(2) Imrie, C. T. *Trends Polym. Sci.* **1995**, *3*, 22.
(3) Bazuin, C. G.; Tork, A. *Macromolecules* **1995**, *28*, 8877.
(4) Brandys, F. A.; Bazuin, C. G. *Chem. Mater.* **1996**, *8*, 83.
(5) Antonietti, M.; Conrad, J.; Thünemann, A. *Macromolecules* **1994**, *27*, 6007.
(6) Kato, T.; Fréchet, J. M. J. *Macromolecules* **1989**, *22*, 3819.
(7) Ikkala,O.; Ruokolainen, J.; ten Brinke, G.; Torkkeli, M.; Serimaa, R. *Macromolecules* **1995**, *28*, 7088.
(8) Ruokolainen, J.; Tanner, J.; ten Brinke, G.; Ikkala,O.; Torkkeli, M.; Serimaa, R *Macromolecules* **1995**, *28*, 7779.
(9) Ruokolainen, J.; ten Brinke, G.; Ikkala, O.; Torkkeli, M.; Serimaa, R. *Macromolecules* **1996**, *29*, 3409.
(10) Ruokolainen, J.; Torkkeli, M.; Serimaa, R.; Vahvaselkä, S.; Saariaho, M.; ten Brinke, G.; Ikkala, O. *Macromolecules* **1996**, *29*, 6621.
(11) Ten Brinke, G.; Ruokolainen, J.; Ikkala, O. *Europhys. Lett.* **1996**, *35*, 91.
(12) Ruokolainen, J.; Torkkeli, M.; Serimaa, R.; Komanschek, B. E.; Ikkala, O.; ten Brinke, G. *Phys. Rev. E* **1996**, *54*, 6646.
(13) De Gennes, P.-G. *Scaling Concepts in Polymer Physics*; Cornell University Press: Ithaca, NY, 1979.
(14) Leibler, L. *Macromolecules* **1980**, *13*, 1602.
(15) Benoit, H.; Hadziioannou, G. *Macromolecules* **1988**, *21*, 1449.
(16) Walker, J. S.; Vause, C. A. *J. Chem. Phys.* **1983**, *79*, 2660.
(17) Walker, J. S.; Vause, C. A. *Sci. Am.* **1987**, *256* (5), 90.
(18) Ten Brinke, G.; Karasz, F. E. *Macromolecules* **1984**, *17*, 815.
(19) Sanchez, I. C.; Balasz, A. C. *Macromolecules* **1989**, *22*, 2325.
(20) Rowlinson, J. S.; Swinton, F. L. *Liquids and Liquid Mixtures*; Butterworth Scientific: London, 1982.
(21) Davis, H. T. *Statistical Mechanics of Phases, Interfaces and Thin Films*; VCH Publishers: New York, 1996.
(22) Wall, F. T.; Mandel, F. *J. Chem. Phys.* **1975**, *63*, 4592.
(23) Metropolis, N.; Rosenbluth, A. W.; Rosenbluth, M. N.; Teller, A. H.; Teller, E. *J. Chem. Phys.* **1953**, *21*, 1087.
(24) Huh, J., unpublished results.
(25) Foster, D. P.; Jasnow, D.; Balazs, A. C. *Macromolecules* **1995**, *28*, 3450.
(26) Khalatur, P. G.; Khokhlov, A. R. *Macromol. Theory Simul.* **1996**, *5*, 877.
(27) Ikkala, O.; Ruokolainen, J.; Torkkeli, M.; Serimaa, R.; ten Brinke, G. *Macromol. Symp.* (European Polymer Blend Meeting, Maastricht, 1996), in press.
(28) Inomata, K.; Haraguchi, M.; Nose, T. *Polymer* **1996**, *37*, 4223.
(29) Huh, J., unpublished results.
(30) Tanaka, F.; Ishida, M. *Macromolecules*, in press.
(31) Tanaka, F.; Ishida, M.; Matsuyama, A. *Macromolecules* **1991**, *24*, 5582.
(32) Tanaka, F. *Adv. Colloid Interface Sci.* **1996**, *63*, 23.

MA9614398